

Multi-Nucleation-Based Formation of Oriented Zinc Oxide Microcrystals and Films in Aqueous Solutions

Shingo Hirano,* Kyosuke Masuya, and Makoto Kuwabara

Department of Materials Engineering, Graduate School of Engineering, University of Tokyo, 7-3-1 Hongo, Bunkyo-ku, Tokyo 113-8656, Japan

Received: December 25, 2003

A wet-chemical deposition method of synthesizing highly oriented, transparent ZnO films on a crystalline template is described. Multi-nucleation and the subsequent growth of ZnO nanodomains at an early stage of wet-chemical deposition leads to the formation of thin hexagonal platelike ZnO crystals spread over the template film. A subsequent temperature increase allows the growth of oriented rods, whose size depends on that of the platelike crystals. Consequently, oriented ZnO films with various microstructures can be synthesized by controlling the size of the ZnO plates at an early stage of deposition.

ZnO possesses unique electrical and optical properties that have many important applications, such as in transparent conducting films, waveguides, ultraviolet lasers, etc. The low-dimensional structure of ZnO is important for optical applications such as lasers;¹ the solution chemistry-based route, which provides various size- and morphology-controlled nanocrystals, has focused on synthesizing nanostructured ZnO.^{2–5} Furthermore, in contrast to high temperature processes, chemical deposition methods have recently received more attention because of interest in developing low-temperature, large-scale production of nanostructured ZnO films.^{6–8} To control the surface density, the orientation and size of ZnO nanorods on various substrates remain important challenges for realizing various industrial applications.

This paper describes the multi-nucleation-based growth of highly oriented zinc oxide (ZnO) microcrystals and films on a ZnO template, using a wet-chemical approach, which is a significant advance in synthesizing well-oriented, dense, thick films. Our method is characterized by the formation of thin hexagonal platelike ZnO crystals spread over the template film at an early stage of wet-chemical deposition, which is associated with the growth of nanocrystalline domains via multi-nucleation. A subsequent temperature increase allows the growth of oriented rods dependent on the platelike crystals, i.e., the size of the rods depends on that of the platelike crystals. Consequently, oriented ZnO films with various microstructures can be synthesized by controlling the size of the plates at an early stage of deposition.

Figure 1 shows the evolution of the microstructure of the surface of a polycrystalline ZnO template film⁹ (~80 nm thick) as a function of reaction temperature, when the reaction vessel containing the template film and an aqueous solution of 0.1 M zinc nitrate and hexamethylenetetramine (HMT) was heated to 77 °C at a rate of 0.3 °C/min. Immediately after the reaction temperature reached 40, 50, 56, 64, 67, 72, and 77 °C, the reaction was quenched by cooling the vessel in an ice bath. Then, the samples were cleaned ultrasonically for 5 min in distilled water to remove any precipitate attached to the surface of the deposited films. The effect of ZnO template films on the

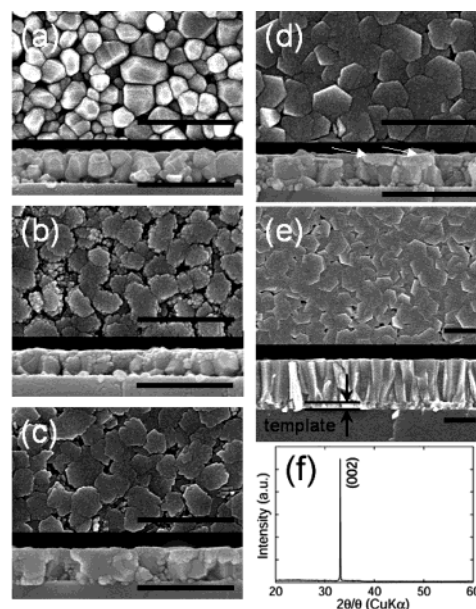


Figure 1. SEM images of samples deposited at various temperatures in aqueous solutions containing 0.1 M zinc nitrate and HMT; top view and cross-sectional view of (a) ZnO template film and films deposited at (b) 40, (c) 50, (d) 56, and (e) 77 °C. (Bars = 500 nm.) (f) The out-plane XRD pattern for the film deposited at 77 °C shows that the *c*-axis of ZnO crystals is preferentially oriented perpendicular to the plane of the substrate.

formation of ZnO nanorods has been discussed previously.^{7,8} As shown in Figure 1(a), the ZnO template film has a porous polycrystalline microstructure, and XRD studies for the templates revealed that the *c*-axis of ZnO crystals is preferentially oriented perpendicular to the plane of the substrate. As the temperature increases to 56 °C, the agglomerates gradually transform into ~40-nm-thick hexagonal platelike crystals [see Figures 1(b) and (c)]. At 56 °C, the hexagonal platelike crystals formed on top of the template cover the initially porous template completely. At these stages, the growth of platelike crystals in the direction lateral to the template film (i.e., the *a*-axis direction of ZnO) is conspicuous, and lateral growth is constrained by contact between adjacent platelike crystals; as a result, a dense

* Author to whom all correspondence should be addressed. E-mail: hirano@material.t.u-tokyo.ac.jp.

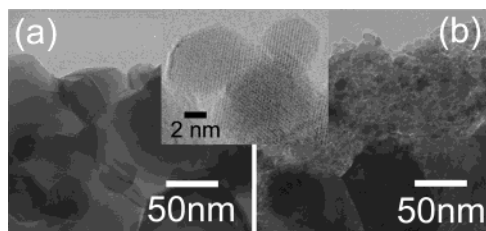


Figure 2. TEM images for the edge of (a) the template and (b) a thin film deposited in a solution containing 0.1 M zinc nitrate and HMT at a heating rate of 0.3 °C/min and 40 °C. The inset shows a lattice image of nanodomains deposited on the template at a heating rate of 0.3 °C/min and 50 °C. In Figure 3(b), large crystalline particles show grains of the template.

surface layer consisting of platelike crystals appears. This cannot be interpreted by the previous findings that ZnO tends to grow into hexagonal rod structures along the $\langle 00l \rangle$ axis, but is similar to the case that ZnO nanorods consisting of nanoplates (~ 15 nm thick) form in the presence of a template.¹⁰ At temperatures from ~ 60 to 80 °C, growth in the direction vertical to the template is observed, which leads to a dense, well-crystallized ZnO film about 700 nm thick [Figure 1(e)] and good optical transparency in the visible range (see Supporting Information). In comparison with previously reported ZnO films composed of nanorods,^{6–8} our thick film has a dense microstructure and smooth surface. It is generally difficult to synthesize such oriented, dense, thick oxide films at a temperature as low as 100 °C. XRD studies revealed that these thick films show strong diffraction derived from the $\langle 00l \rangle$ planes [see Figure 1(f)], in which the degree of $\langle 00l \rangle$ orientation (F_{00l}) calculated using Lotgering's method reached 0.99,¹¹ which is higher than that calculated from the XRD patterns of recently reported films composed of ZnO nanorods ($F_{00l} \sim 0.21$ – 0.48).^{6,7} The $\langle 00l \rangle$ orientation behavior did not change at any stage of deposition, and the intensity of the $\langle 00l \rangle$ diffraction peak increased with the reaction temperature (see Supporting Information).

Figure 2 shows TEM images of the edge of the template and a thin film deposited at 40 °C. The grains of the template have a smooth surface, whereas an inhomogeneous, finer microstructure appears on the template after deposition, which agrees with SEM observations [see, Figure 1(b)]. The low contrast between crystalline regions in the deposited film indicates that space separates adjacent nanocrystalline domains. Figures 3 shows cross-sectional TEM images of a thin film deposited at 50 °C. In Figure 3(b), an amorphous layer (~ 5 nm thick) is observed between the template and the Si, which might be derived from a Si–O compound. Moreover, this high-resolution image shows that the c -axis of the template grains is preferentially oriented perpendicular to the plane of the substrate, which is in good agreement with the results of the XRD measurements. However, we observed that the c -axis of some grains was tilted toward the substrate plane by from a few to more than 10 degrees. As shown in Figure 3(c), nanocrystalline domains were observed near the surface of the deposited film; however, the lattice planes were roughly aligned and parallel to the lattice planes of the grain of the template, which suggests that the deposited film grew epitaxially on the template. Furthermore, regions with small-angle grain boundaries indicated misorientations between domains in the c -axis direction [Figure 3(d)].

The formation of the nanodomain structure could be explained by either multi-nucleation with subsequent growth via monomers or oriented aggregation via dispersed nanoparticles. There has been extensive research on the latter recently,^{3,12–14} such misorientations are also generated by imperfectly oriented attachment between nanoparticles. For a colloidal solution

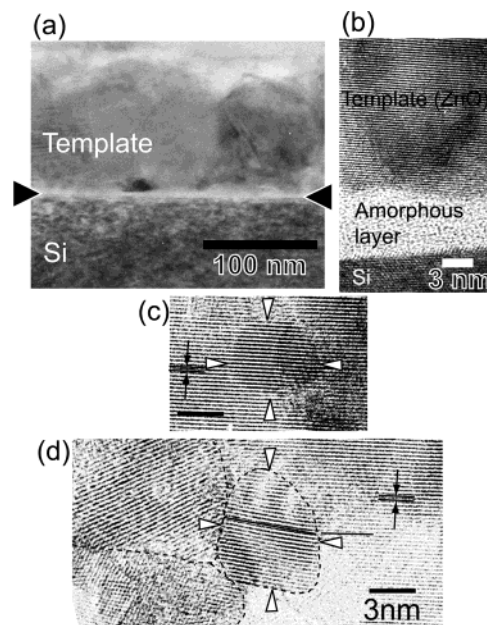


Figure 3. High-resolution (HR) bright-field TEM images of a cross-section of an oriented ZnO film deposited at a heating rate of 0.3 °C/min and 50 °C; (a) a low magnification image of the cross-section, and (b) a high-resolution image near the interface between the Si and a grain of the template. In Figure 3(a), the arrowheads indicate an amorphous layer on the Si. Figures 3(c) and 3(d) show the microstructure near the surface of the deposited film. In Figures 3(c) and 3(d), the arrowheads indicate nanodomains. The arrows indicate a lattice spacing of ~ 2.6 Å, which corresponds to the $\langle 002 \rangle$ planes of the Wurtzite structure. In Figure 3(d), the lattice planes are highlighted for clarity. (Bars = 3 nm.)

containing ZnO nanoparticles, aggregation-based growth clearly gives rise to the formation of large ZnO rods.³ Therefore, to examine the growth behavior, we investigated the dispersion and size of particles in solutions using absorption spectra and high-resolution dynamic light scattering (DLS) measurements (see Supporting Information). The absorption spectra of solutions heated at 40 and 50 °C did not show the fundamental absorption edge of ZnO, which indicates that well-dispersed nanoparticles do not exist in solutions at low temperature. The DLS data indicated that there were no nanoparticles of a few nanometers in size, although there were large crystals averaging > 100 nm in diameter. To examine these data for aqueous solutions, we conducted TEM observations for the precipitated powder collected from 0.1 M aqueous solutions heated at various temperatures. Large aggregates of ZnO nanoparticles were seen in the aqueous solution heated to 67 °C [Figure 4(b), average primary particle diameter: ~ 8 nm], in addition to needlelike ZnO particles [e.g., at 50 °C, these were ~ 400 nm long and ~ 70 nm in diameter, Figure 4(a)]. This behavior appears to contradict the conclusion that ZnO nanoparticles do not exist in aqueous solutions. Rather, the nanoparticles exist in solution, but tend to form large aggregates. More importantly, the electron diffraction patterns of these aggregates showed a Debye–Scherrer ring, which indicates that there was no crystallographic orientation between the nanoparticles [see inset of Figure 4(b)]. This suggests that an overall oriented aggregation does not occur, although the nanoparticles exist in aqueous solutions. This behavior might occur if the solutions are not stable colloidal suspensions, i.e., rapid aggregation might prevent particles from rotating sufficiently for oriented attachment. These aggregates of ZnO nanoparticles were also observed for solutions heated to 50 °C, which suggests that the size of nanoparticles in large aggregates does not change even if large ZnO crystals grow in

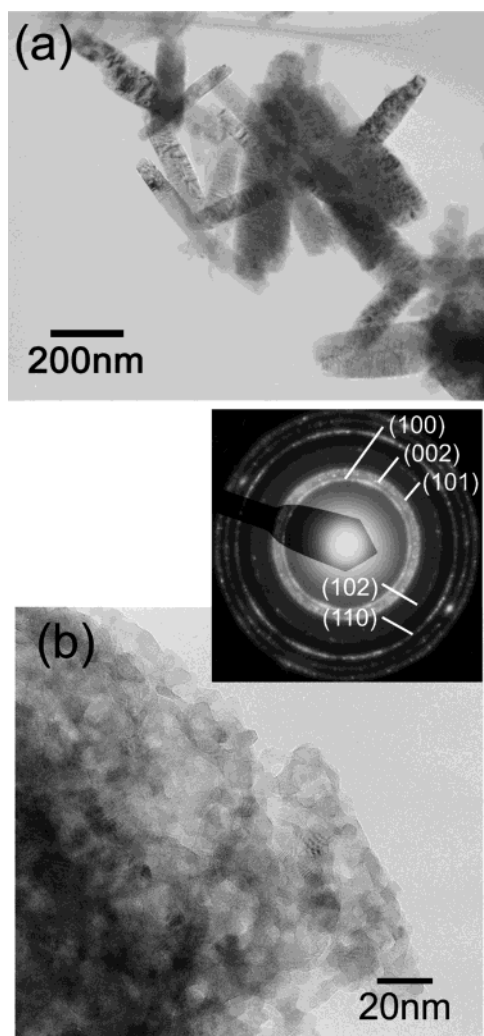


Figure 4. Bright-field TEM images of powders formed in 0.1 M aqueous solutions heated to (a) 50 and (b) 67 °C. The inset of Figure 4(b) shows the electron diffraction (ED) pattern, which corresponds to this figure. This ED pattern reveals that the particles are in a single phase of ZnO with the Wurtzite structure.

the same solution. Furthermore, as seen in Figure 4(a), the particles precipitated homogeneously in aqueous solutions were needlelike, and unlike the hexagonal platelike crystals formed on the template. This behavior might have been due to differences in the growth process; i.e., the hexagonal platelike crystals grew epitaxially on relatively large grains of the template, while the needlelike crystals grew gradually from homogeneously dispersed nuclei in the solutions.

Considering the above-mentioned (00 l) orientation behavior of the deposited films, these results indicate that the nanocrystalline domains form via multi-nucleation and subsequent growth on crystals rather than via the oriented aggregation of dispersed nanoparticles. As the growth rate is slow at low temperatures, this behavior might occur with nucleation and two-dimensional growth of nanodomains on the template and newly formed nanodomains, leading to the formation of platelike crystals.

Misorientation between nanodomains might originate from misoriented nucleation at the surface of crystals. As the reaction temperature increases, ZnO crystals rapidly grow vertically with respect to the substrate, which leads to an oriented film consisting of rodlike crystals.

If this model is applicable to our system, the temperature and number of ions are essential factors controlling the formation of platelike crystals. When the solution containing 0.1 M zinc ions was heated more rapidly (~ 1 °C/min), or when the concentration of zinc ions and the heating rate were low (e.g., 0.005 M and 0.3 °C/min, respectively), smaller platelike crystals were observed on the template; i.e., crystal growth lateral to the surface of the template was inhibited, leading to the open structure of the deposited films (see Supporting Information). These results indicate that low-temperature aging using high-concentration solutions is effective for forming large platelike crystals, and the size of the ZnO plates determines the size of the oriented ZnO rods. Note that the observed growth process produces well-crystallized oxide films at low temperatures. Therefore, this process is exceedingly important as a novel synthesis route for dense oxide films on various template materials. This method will be applicable for fabricating various nanostructured ZnO devices.

Acknowledgment. The authors gratefully thank Y. Ikuhara and T. Yamamoto (DME, University of Tokyo), H. Tsunakawa, T. Moroyama, T. Ito, and Y. Kakegawa (IEI, University of Tokyo), T. Suga and M. R. Howlander (RCAT, University of Tokyo) for the support of TEM facilities. The authors also thank K. Tanaka (Otsuka Electronics) for the support of DLS measurements.

Supporting Information Available: Synthesis and results of characterization. This material is available free of charge via the Internet at <http://pubs.acs.org>.

References and Notes

- (1) Huang, M. H.; Mao, S.; Feick, H.; Yan, H.; Wu, Y.; Kind, H.; Weber, E.; Russo, R.; Yang, P. *Science* **2001**, *292*, 1897–1899.
- (2) Spanhel, L.; Anderson, M. A. *J. Am. Chem. Soc.* **1991**, *113*, 2826–2833.
- (3) Pacholski, C.; Kornowski, A.; Weller, H. *Angew. Chem., Int. Ed.* **2002**, *41*, 1188–1191.
- (4) Vergés, M. A.; Mifsud, A.; Serna, C. J. *J. Chem. Soc., Faraday Trans.* **1990**, *86*, 959–963.
- (5) Liu, B.; Zeng, H. C. *J. Am. Chem. Soc.* **2003**, *125*, 4430–4431.
- (6) Vayssieres, L.; Keis, K.; Lindquist, S.-E.; Hagfeldt, A. *J. Phys. Chem. B* **2001**, *105*, 3350–3352.
- (7) Boyle, D. S.; Govender, K.; O'Brien, P. *Chem. Commun.* **2002**, 80–81.
- (8) Yamabi, S.; Imai, H. *J. Mater. Chem.* **2002**, *12*, 3773–3778.
- (9) Ohyama, M.; Kozuka, H.; Yoko, T. *Thin Solid Films* **1997**, *306*, 78–85.
- (10) Tian, Z. R.; Voigt, J. A.; Liu, J.; McKenzie, B.; McDermott, M. J. *J. Am. Chem. Soc.* **2002**, *124*, 12954–12955.
- (11) Lotgering, F. K. *J. Inorg. Nucl. Chem.* **1959**, *9*, 113–123.
- (12) Penn, R. L.; Banfield, J. F. *Science* **1998**, *281*, 969–971.
- (13) Penn, R. L.; Oskam, G.; Strathmann, T. J.; Searson, P. C.; Stone, A. T.; Veblen, D. R. *J. Phys. Chem. B* **2001**, *105*, 2177–2182.
- (14) Banfield, J. F.; Welch, S. A.; Zhang, H.; Ebert, T. T.; Penn, R. L. *Science* **2000**, *289*, 751–754.